

Structural and Functional Mapping of Mesenchymal Bodies

Sébastien Sart^{1,2}, Raphaël F.-X.Tomasi^{1,2}, Antoine Barizien^{1,2},
Gabriel Amselem¹, Ana Cumano^{3,4} and Charles N. Baroud^{1,2,*}

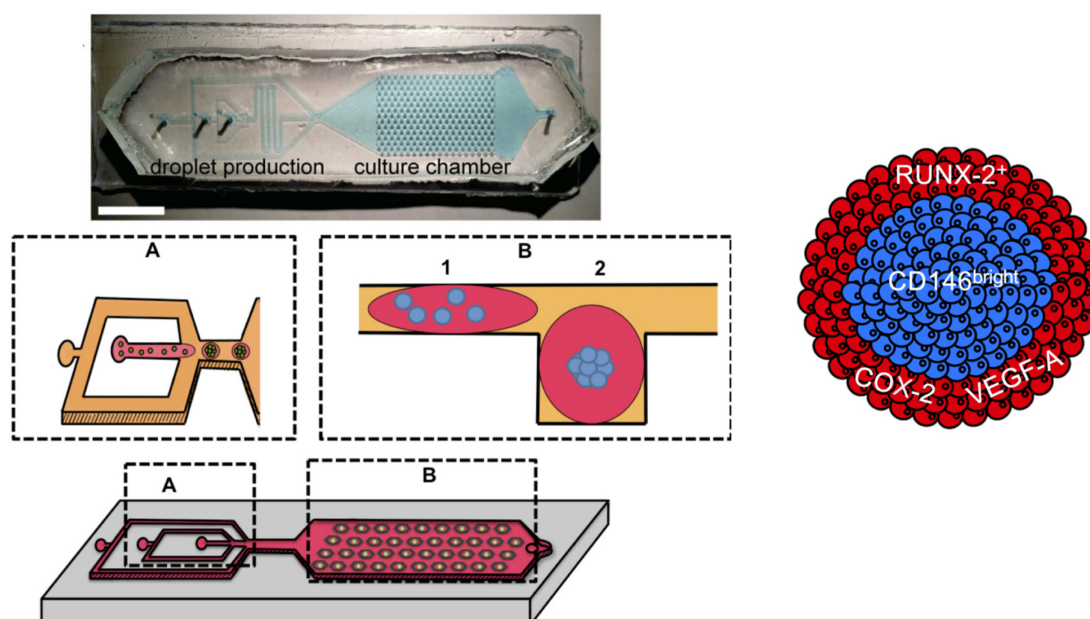
¹LadHyX and Department of Mechanics, Ecole Polytechnique CNRS - UMR 7646, Palaiseau, France;

²Physical Microfluidics and Bio-Engineering, Department of Genomes and Genetics, Institut Pasteur, Paris, France; ³Unit for Lymphopoiesis, Department of Immunology – INSERM U1223, Institut Pasteur, Paris, France; ⁴Université Paris Diderot, Sorbonne Paris Cité, Cellule Pasteur, 75018, Paris, France

*For correspondence: charles.baroud@pasteur.fr

[Abstract] The formation of spheroids with mesenchymal stem/stromal cells (MSCs), mesenchymal bodies (MBs), is usually performed using bioreactors or conventional well plates. While these methods promote the formation of a large number of spheroids, they provide limited control over their structure or over the regulation of their environment. It has therefore been hard to elucidate the mechanisms orchestrating the structural organization and the induction of the trophic functions of MBs until now. We have recently demonstrated an integrated droplet-based microfluidic platform for the high-density formation and culture of MBs, as well as for the quantitative characterization of the structural and functional organization of cells within them. The protocol starts with a suspension of a few hundred MSCs encapsulated within microfluidic droplets held in capillary traps. After droplet immobilization, MSCs start clustering and form densely packed spherical aggregates that display a tight size distribution. Quantitative imaging is used to provide a robust demonstration that human MSCs self-organize in a hierarchical manner, by taking advantage of the good fit between the microfluidic chip and conventional microscopy techniques. Moreover, the structural organization within the MBs is found to correlate with the induction of osteo-endocrine functions (*i.e.*, COX-2 and VEGF-A expression). Therefore, the present platform provides a unique method to link the structural organization in MBs to their functional properties.

Graphic abstract:



Droplet microfluidic platform for integrated formation, culture, and characterization of mesenchymal bodies (MBs). The device is equipped with a droplet production area (flow focusing) and a culture chamber that enables the culture of 270 MBs in parallel. A layer-by-layer analysis revealed a hierarchical developmental organization within MBs.

Keywords: Mesenchymal stromal cells, Mesenchymal bodies, Microfluidics, Droplets, Spheroids, Quantitative imaging

[Background] Mesenchymal stem/stromal cells (MSCs) comprise a heterogeneous population of mesenchymal progenitors that are capable of differentiation into osteoblastic, chondrogenic, and adipogenic lineages (Dominici *et al.*, 2006). MSCs also bear important trophic functions that regulate immune cell activities, promote angiogenesis, reduce tissue inflammation, and activate tissue-resident progenitors, making this cell type particularly suited for many tissue engineering/regeneration applications (Caplan and Correa, 2011). The formation of spheroids with MSCs (*i.e.*, mesenchymal bodies, MBs) was recently found to enhance their differentiation potential and their secretory activities (Sart *et al.*, 2014). However, it remains poorly understood how heterogeneous hMSCs self-organize in 3D, as well as the mechanisms linking their structural organization to their functional activities (Cesarz and Tamama, 2016).

Several methods have been used for the formation of MBs, including bioreactors and conventional well plates (Sart *et al.*, 2014 and 2016; Sart and Agathos, 2018). However, while these methods enable the formation of a large number of MBs, they provide limited control over single aggregate stimulation or characterization (Sart *et al.*, 2016; Sart and Agathos, 2018). Because MSCs constitute a heterogeneous population, the analysis of single aggregates at single-cell resolution is required to

understand the mechanisms by which 3D cultivation induces functional changes on the behavior of a minority of very responsive cells or a global population shift. The macro-scale culture vessels and global population analysis therefore do not allow the MB structure and the cellular functions to be related (Sart *et al.*, 2017; Sart and Agathos, 2018).

Here, we use a microfluidic platform that allows high density and controlled-sized MB formation within nanoliter drops. The microfluidic format enables a robust quantitative demonstration, using quantitative imaging at a single-cell level, that human MSCs self-organize in a hierarchical manner: The most undifferentiated MSCs are located in the core, while partially committed cells are located at the boundaries of the MBs. Moreover, we found that such structural organization correlated with the induction of osteo-endocrine functions. The microfluidic method and protocols developed here can find applications to characterize other types of organoids, to link cell sorting processes to phenotypic commitment, in view of understanding the mechanisms leading to tissue patterning in 3D stem cell cultures. The current method can be applied to any kind of stem cells cultivated in 3D, although the volume of droplets should be adapted to a specific type of stem cells. The data-driven approach developed in this protocol allows us to obtain a robust quantitative characterization of the structural and functional organization within organoids, which would be difficult to obtain using conventional population-based approaches that require the alteration of the cellular microenvironment.

Materials and Reagents

A. Cell culture reagents

1. T-175 cm² flasks (Greiner, Cellstar, catalog number: 660175)
2. Human mesenchymal stromal cells derived from the Wharton's jelly of the umbilical cord (hMSCs), purchased from American Type Culture Collection (ATCC) (ref #PCS-500-010)
3. α -modified Eagle's medium (α -MEM) (Life Technologies, catalog number: 32561-029)
4. TrypLE™ Express (Life Technologies, catalog number: 12604013)
5. Phosphate buffer saline (PBS) (Sigma-Aldrich, catalog number: D8662)
6. Fetal bovine serum (FBS) (Life Technologies, catalog number: 10500-064)
7. Penicillin- streptomycin (pen-strep) (Life Technologies, catalog number: 10378-016)
8. Triton X-100 (Sigma-Aldrich, catalog number: X100)
9. Ultra-low-melting agarose (Sigma-Aldrich, catalog number: A5030)
10. Paraformaldehyde (PFA), 16% (Alpha Aesar, catalog number: 43368)
11. Mouse anti-human CD146-Alexa Fluor 647 (clone P1-H12) (BD Biosciences, catalog number: 563619)
12. Rabbit anti-COX-2 polyclonal antibody (Abcam, catalog number: ab15191)
13. Rabbit anti-human VEGF-A monoclonal antibody (Abcam, catalog number: ab52917)
14. Mouse anti-human RUNX-2 monoclonal antibody (Abcam, catalog number: ab76956)
15. Alexa Fluor 488-conjugated goat anti-mouse IgG2a secondary antibody (Life Technologies, catalog number: A-21131)

16. Alexa Fluor 594-conjugated goat polyclonal anti-rabbit IgG secondary antibody (Life Technologies, catalog number: A-11012)
17. DAPI (Sigma-Aldrich, catalog number: 10236276001)
18. Vybrant™ multicolor cell labeling kit (Life Technologies, catalog number: V22889)
19. hMSC culture medium (see Recipes)
20. Staining buffer (see Recipes)
21. CD146 staining solution (see Recipes)
22. Fixative solution (see Recipes)
23. Agarose solution (see Recipes)
24. Permeabilization buffer (see Recipes)
25. Blocking buffer (see Recipes)
26. Primary antibodies solution (see Recipes)
27. Secondary antibodies solution (see Recipes)

B. Materials for microfabrication and microfluidics

1. Brass plates (5 × 5 cm)
2. Dry-film photoresists: Eternal Laminar E8020, Eternal Laminar E8013 (Eternal Materials), and Alphi NIT215 (Nichigo-Morton)
3. K₂CO₃ (Sigma-Aldrich, catalog number: P5833)
4. Poly(dimethylsiloxane) (PDMS) (Dow Corning, catalog number: SYLGARD 184)
5. 3M™ Novec™ 1720 Electronic Grade Coating (3M)
6. 3M™ Fluorinert™ Electronic Liquid FC-40 (3M)
7. PEG-di-Krytox (RAN Biotechnologies)

Equipment

A. Equipment for cell culture

1. CO₂ incubator (Binder, CB 170)
2. Cell sorter (flow cytometer) (BD Biosciences, FACSAria III)

B. Equipment for microfabrication and microfluidics

1. Office laminator (PEAK, pro PS320)
2. Ultraviolet lamp (Hamamatsu, Lightningcure)
3. Micromilling machine (Minitex Machinery, CNCMini-Mill/GX)
4. Plasma cleaner (Harric, PDC-32G)
5. 100 µl and 1 ml glass syringes (SGE, Analytical Science, Gas tight luer lock syringes)
6. 1 ml plastic syringe (Terumo, SS+01T1)
7. Syringe pumps (neMESYS Low-Pressure Syringe Pump, Cetoni GmbH)

C. Microscopy

1. Motorized wide-field microscope (Ti, Eclipse, Nikon), equipped with a CMOS (complementary metal-oxide semiconductor) camera (ORCA-Flash4.0, Hamamatsu), a fluorescence light-emitting diode source (Spectra X, Lumencor), and a 10× objective with a 4-mm working distance (extra-long working distance) and a 0.45 numerical aperture (NA) (Plan Apo λ, Nikon)
2. Motorized (Ti2, Nikon) confocal spinning disc microscope equipped with lasers (W1, Yokogawa) and the same camera and objective as above

Software

1. MATLAB (r2016a, MathWorks, Natick, MA)

Procedure

A. Microfabrication of the microfluidic chips

1. A detailed protocol on the fabrication of the chips can be found in Amselem *et al.* (2018). The chips consist of two parts: 1) The top part comprises a flow focusing junction, a serpentine, diverging rails, and a culture chamber. The molds are fabricated using dry resins that are etched to produce the shape of the droplet generators and guiding channels by standard soft lithography. 2) The bottom of the chips consists of an array of 270 hexagonal capillary traps. The molds of the bottoms part of the chips are fabricated by micromilling the brass plates. The geometry and dimensions of the features can be found in Sart *et al.* (2020) (**Figure 1**).

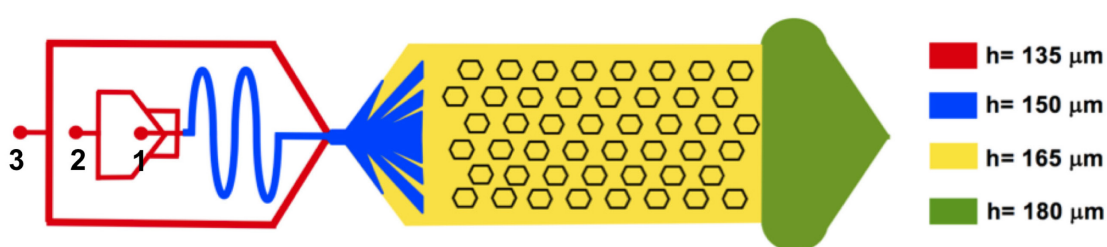


Figure 1. Chip design and depth of the different regions. 1. Inlet for the injection of the aqueous phase containing cells and culture medium; 2. Inlet for oil injection at the junction; 3. Inlet for oil injection to push the drops within the trapping chamber.

2. Fabricate the tops and the floors of the chips by casting poly(dimethylsiloxane) (PDMS) (a mix of 90% of base and 10% of curing agents) into the molds.
3. Place the two molds in an oven set up at 80°C for 2 h to promote the polymerization of the PDMS.
4. Extract the two parts of the chips from the molds and cut them with a scalpel.

5. Assemble the two parts of the chips by bonding the two surfaces for 40 s using a plasma cleaner.
6. Flush the chips with Novex and heat them at 110°C for three cycles to render the inner walls of the chip fluorophilic.

B. Cell culture, sorting, and loading in microfluidic droplets

1. Cultivate hMSCs using hMSC culture medium, from passage 2 to 7 in regular T-175 cm² flasks, and place them into a culture incubator, set up at 37°C and 5% CO₂.
2. Seed the cells into the flask at a density of 5 × 10³ cells/cm², subcultivate them every week using TrypLE, and change the medium every 2 days.

Optionally, sort hMSCs based on their level of expression of CD146 by flow cytometry. CD146 is a marker of undifferentiated status, whose level of expression decreases upon differentiation (Sacchetti *et al.*, 2007). To separate the CD146^{dim} and CD146^{bright} hMSCs, isolate the cells (passage 5) from the flasks, and incubate them with CD146 staining solution for 30 min. Wash the cells with straining buffer. Identify and select the hMSC population by plotting FSC-A and SSC-A signals using the flow cytometer. Eliminate cell doublets by gating the main population obtained by plotting FSC-H versus FSC-A signals. From this selected population, plot the FITC-A (or any fluorochrome for which the cells are not labeled) versus Alexa-647-A signal distribution; analyze the spread of expression of CD146 with the cytometer and sort 25% of the brightest and 25% of the dimmest cells.

3. Connect two 1 ml syringes containing a 1% RAN in FC-40 solution to inlets #3 and #2, block inlet #1, then flush the oil of each syringe at 50 µl/min to remove the air from the chip (**Figure 2, Step 1**).
4. Load a suspension of 6 × 10⁶ bulk- or a mix of 50:50 CD146^{dim} and CD146^{bright} sorted- hMSCs/ml in culture medium supplemented with the agarose solution into a 100 µl glass syringe.
5. Connect this syringe into inlet #1 (**Figure 2, Step 2**).
6. Apply a flow rate of 8-8.5 µl/min to syringe 1 and a flow rate of 11 µl/min to syringe 2. The solution containing the cells is pinched at the junction. This yields to the formation of monodispersed droplets containing a suspension of about 380 cells each (**Figure 2, Step 2**).
7. Apply a flow rate of 50 µl/min on syringe 3: the droplets are pushed on the rails that guide them evenly within the culture chamber. The drops are then captured within the capillary traps (**Figure 2, Step 2**).
8. Stop the flow of syringe #1 and apply a flow rate of 100 µl/min to syringes #2 and #3 to remove the excess of non-anchored droplets in the culture chamber (**Figure 2, step 3**).
9. Stop the oil flows; the cells settle down at the bottom of the drops and start clustering.

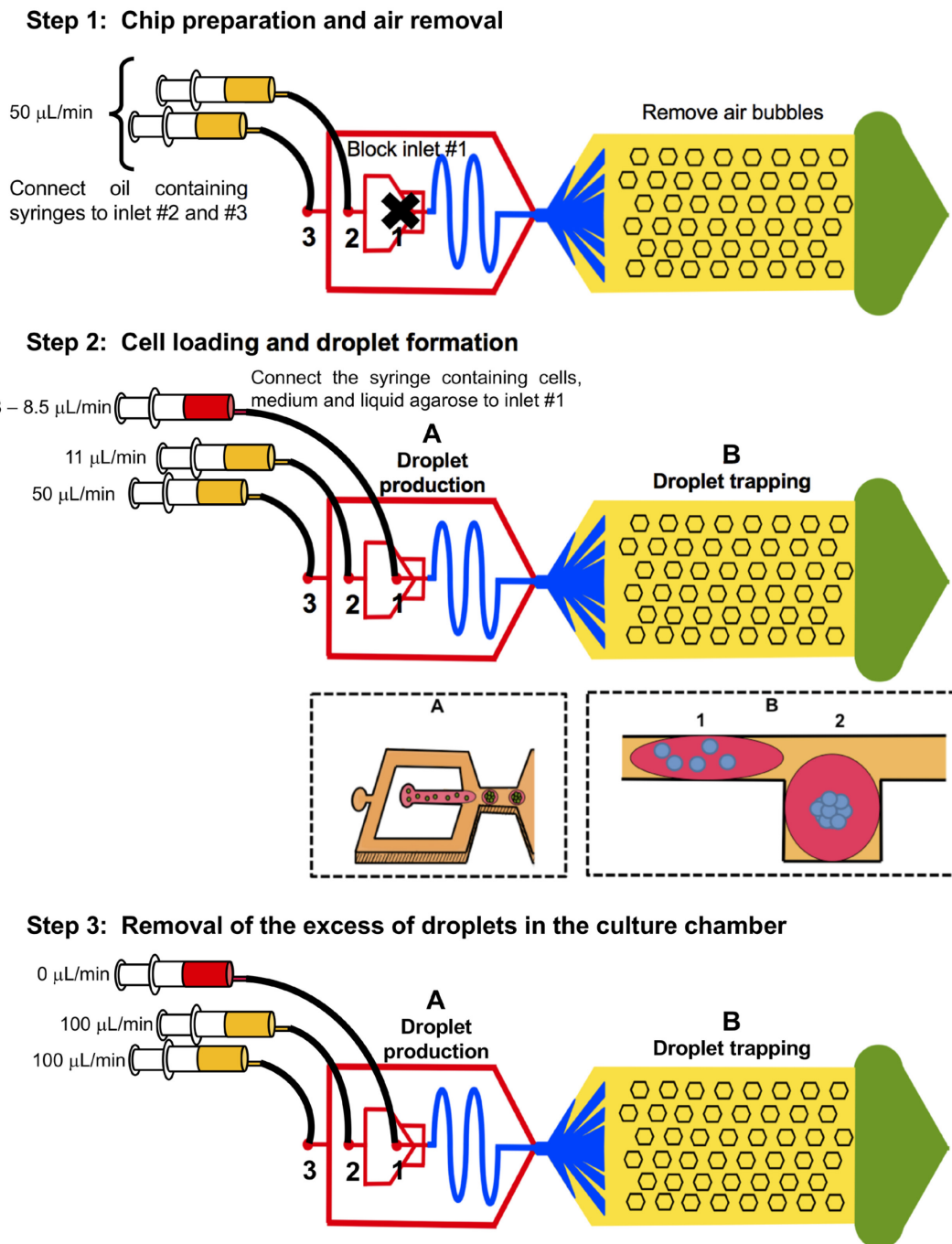


Figure 2. Protocol for cell loading and droplet formation

C. Spheroid formation and culture in microfluidic droplets

1. Place the chips into the CO_2 incubator overnight to let the cells form spheroids (**Figure 3 and Video 1**).

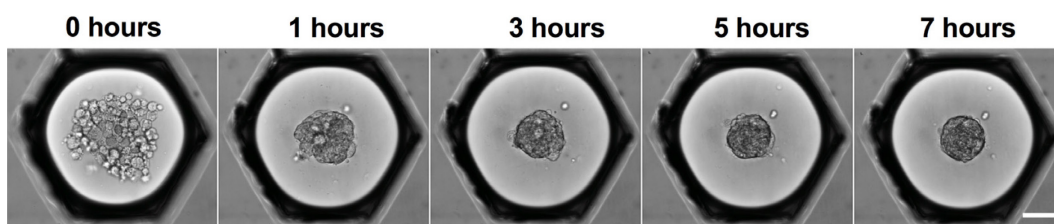
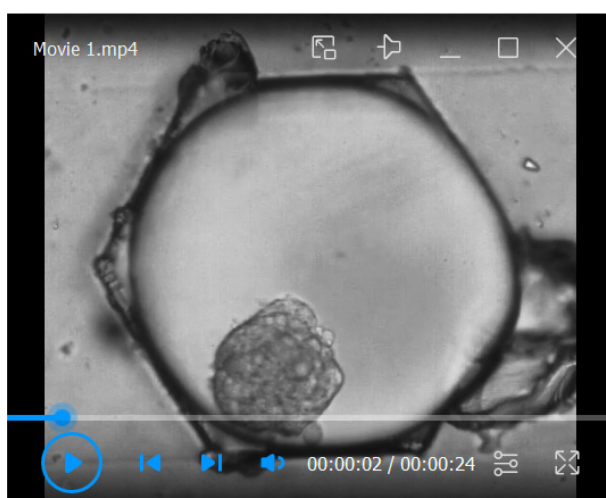


Figure 3. Kinetics of MB formation in microfluidic droplets. After stopping the oil flow, the cells are allowed to settle down to the bottom of the drops, where they start clustering. Cells are monitored continuously by live imaging, while forming MBs. Scale bar = 100 μm .



Video 1. Morphology of MB in 3D. The MBs in liquid drops are subjected to recirculation by applying an oil flow around them. The protocol allows the MBs to rotate on their axis. The movie demonstrates the 3D structural organization of MBs.

2. On the second day, place the chips at 4°C for 30 min to gel the agarose.
3. Flush the chips with 1 ml of pure FC-40 oil, at 80 $\mu\text{l}/\text{min}$, to dilute the surfactant.
4. Replace the oil phase with culture medium by slowly flowing the aqueous solution into the device. At this stage, the 3D aggregates are mechanically retained into the traps by the hydrogel. They can be regularly perfused with culture medium; thus, they are now ready for long-term culture while remaining fully viable (Sart *et al.*, 2020).

D. Spheroid labeling and imaging within microfluidic droplets

To interrogate the structural organization within MBs:

1. Label CD146^{dim-} and CD146^{bright-} hMSCs with Vybrant DiO (green) or Vybrant DiD (red) dyes (5 μl for 1 ml culture medium) for 30 min, prior to loading them into the microfluidic drops.

Note: CD146 protein and the Vybrant dyes are soluble in Triton-X 100 solution; thus, this protocol does not allow to combine immunostaining with the detection of the different CD146 subpopulations.

2. After spheroid formation and culture, image MBs using a fluorescent microscope (e.g., wide-

field or confocal microscope equipped with large working distance objectives) (**Figure 4**).

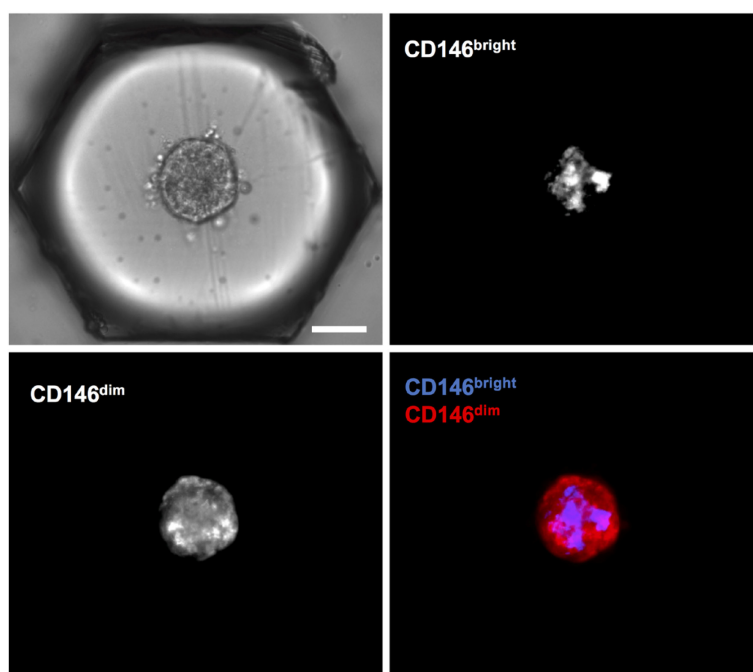


Figure 4. Spatial organization of CD146^{dim} and CD146^{bright} hMSCs within MBs. CD146^{dim} and CD146^{bright} are isolated by cell sorting, then labeled with Vybrant DiO (green) or Vybrant DiD (red) dyes prior to their loading into drops. Scale bar = 100 μ m.

To interrogate the functional organization within MBs (e.g., the regional expression of VEGF-A, COX-2, or RUNX-2):

1. Fix the MBs by perfusing a solution of 200 μ l of fixative solution, by first filling a 1 ml plastic syringe with PFA, then flowing at a flow rate of 80 μ l/min.
2. Incubate the aggregates of hMSCs with the PFA solution for 30 min at room temperature.
3. Wash the culture chamber with PBS at the same flow rate (200 μ l at 80 μ l/min).
4. Permeabilize the MBs by perfusing at 80 μ l/min with a 200 μ l of permeabilization buffer, and incubate for 5 min.
5. Wash the culture chamber with PBS (200 μ l at 80 μ l/min).
6. Block MBs by perfusion of a blocking buffer (200 μ l at 80 μ l/min) and incubate for 30 min.
7. After blocking, perfuse the chamber with a solution of primary antibody (e.g., anti-COX-2 or anti-VEGF-A antibody or anti-RUNX-2; 200 μ l at 80 μ l/min), and incubate for 4 h.
8. Wash the primary antibody solution by perfusing PBS (200 μ l at 80 μ l/min).
9. Perfuse the solution of secondary antibodies (200 μ l at 80 μ l/min) and incubate for 1 h 30 min.
10. Wash with PBS (200 μ l at 80 μ l/min).
11. Image the MBs in the traps using a fluorescent microscope (**Figure 5**).
12. To validate the specificity of the primary antibodies, incubate the sample with the secondary antibody only, then wash with PBS. Absence of fluorescent signal validates that the primary

antibody is specific to its target (*i.e.*, VEGF-A) and that excess of antibodies is effectively washed with PBS rinsing (Sart *et al.*, 2020).

13. To validate the absence of diffusion limitation, omit the blocking step and incubate with the secondary antibody only. Absence of diffusion limitation is demonstrated by homogeneous fluorescent signal distribution within the aggregate (Sart *et al.*, 2020).

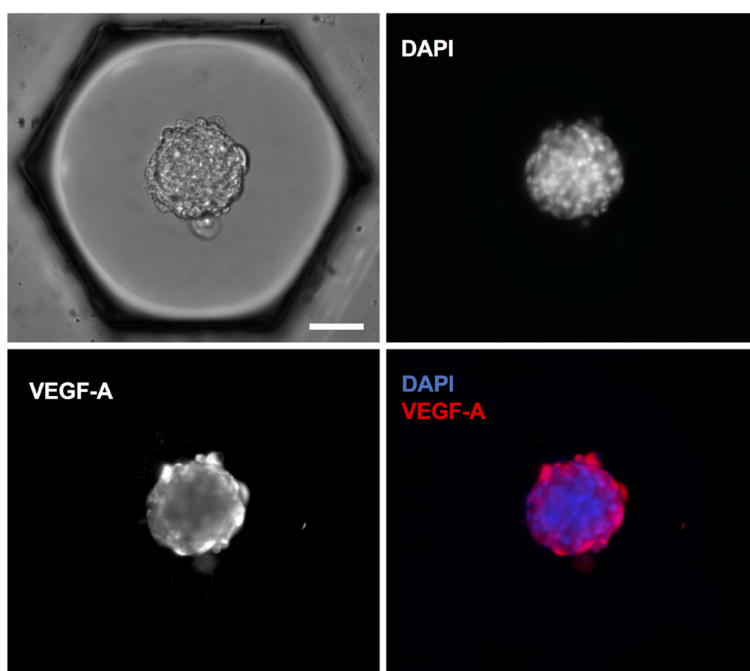


Figure 5. Functional organization hMSCs within MBs: VEGF-A expression detected by immunostaining. Similar results were obtained for RUNX-2 and COX-2 immunostaining (Sart *et al.*, 2020). Scale bar = 100 μ m.

Data analysis

The objective of the data analysis is to provide a quantitative characterization of the structural and functional organization within mesenchymal bodies using image analysis. In the following experiments, the data are generated from about 270 replicates that have been reproduced in at least three different chips.

A. Quantification of the structural organization within MBs using Matlab[®]

Detailed information on data analysis can be found in Sart *et al.* (2017).

1. Identify the centroid of each spheroid.
2. Measure the area (A) of each spheroid.
3. Calculate R, the radius of each spheroid, defined as the square root of A/π .
4. Measure the fluorescent intensity of each pixel of Vybrant DiO (green, corresponding to CD146^{dim} hMSCs) or Vybrant DiD (red, corresponding to CD146^{bright} hMSCs) stained cells, as well as their normalized distance (r/R) to the centroid (**Figures 6A and 6B**).

5. Bin the values of fluorescence at specific (r/R).
6. Normalize the two fluorescent signals against the DAPI signal to take into account the spherical shape of the aggregates.
7. The relative intensity of the two different fluorescence signals indicates the relative abundance of the CD146^{dim} vs. CD146^{bright} hMSCs at different radii within the MBs (**Figure 6C**) (Sart *et al.*, 2020).

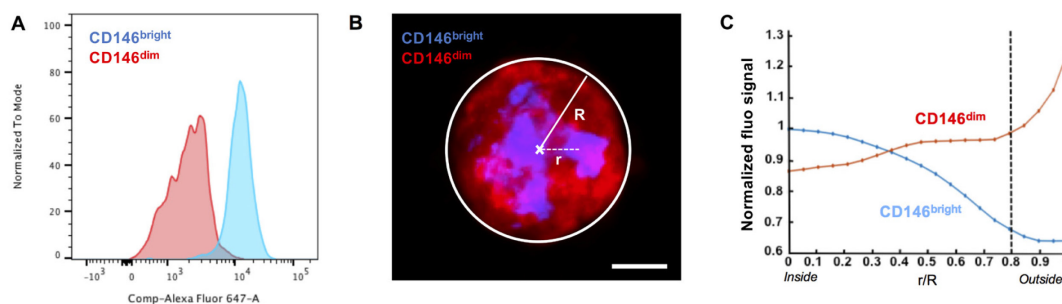


Figure 6. Data analysis methodology to quantify the structural organization in MBs. (A) Cell sorting yielded to the separation of CD146^{dim} and CD146^{bright} populations. (B) Position of the fluorescent signal of CD146^{dim} and CD146^{bright} labeled with Vybrant DiO (green) or Vybrant DiD (red) identified by their radial coordinates (r/R). Scale bar = 100 μ m. (C) Quantification of the distribution of the different CD146 populations within MBs, calculated based on radial coordinates. Part C is extracted from Sart *et al.* (2020).

B. Quantification of the functional organization within MB using Matlab[®]

Detailed information on data analysis can be found in Sart *et al.* (2020):

1. Identify each local maximum of DAPI-stained nuclei (**Figure 7A**).
2. Construct Voronoi diagrams (Chang *et al.*, 2007) by drawing the perpendicular bisectors of the segments between each neighboring local DAPI maxima, which approximate the cell shapes inside the MBs (**Figure 7A**).
3. Identify the position of each layer of cells within the aggregate (**Figure 7B**).
4. Quantify the cellular cytoplasmic fluorescent signal (COX-2, VEGF-A, and RUNX-2) for each cell of the MBs (**Figure 7C**).
5. Correlate the fluorescent signal of each cell to their cell layer position within the MBs (**Figure 7D**). To account for the variability of the cytoplasmic signal across the entire cell (nucleus included), the fluorescence signal of a single cell was defined as the mean signal of the 10% highest pixels of the corresponding Voronoi cell (Sart *et al.*, 2020).
6. Bin the values of fluorescence at specific cell layers.

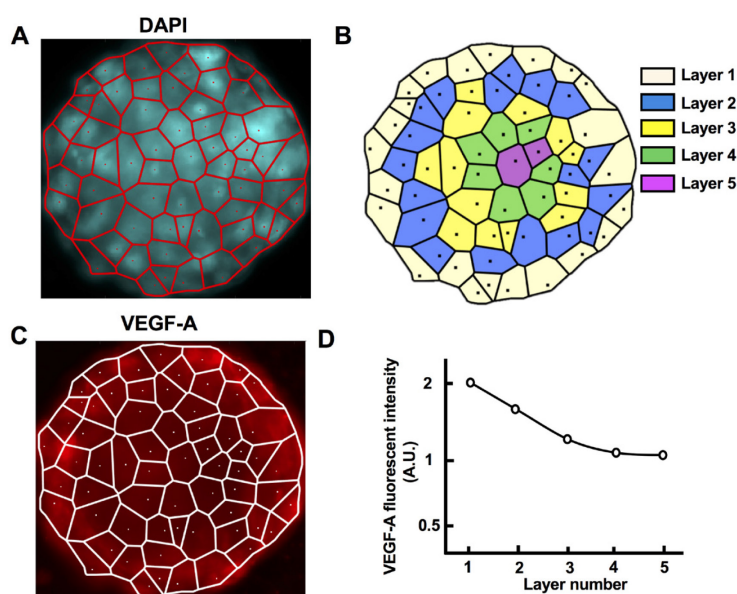


Figure 7. Data analysis methodology to quantify the functional organization in MBs: VEGF-A spatial distribution. (A) Detecting the DAPI signal enables drawing a Voronoi diagram, which allows estimating the area occupied by each cell in the aggregate. (B) The position of each cell is assigned to a layer number. (C) The fluorescent intensity in each cell defined from the Voronoi diagram is measured. (D) The fluorescent intensity of the protein of interest in each cell is correlated to the cell position (layer number) within the MBs, which allows mapping the cell function within the MBs. Similar results were obtained for RUNX-2 and COX-2 immunostaining (Sart *et al.*, 2020).

The results show that hMSCs self-organize in a hierarchical manner: most undifferentiated MSCs are located in the core, while partially committed cells are located at the boundaries of the MBs (**Figure 6**). Moreover, we found that such structural organization correlated with the induction of osteo-endocrine functions (*i.e.*, COX-2 and VEGF-A expression) (**Figure 7** and Sart *et al.*, 2020 for RUNX-2 and COX-2).

Recipes

1. hMSC culture medium
Mix 50 ml of FBS and 5 ml of the pen-strep (100×) with 500 ml of α -MEM basal medium, which results in a medium containing 10% (v/v) FBS and 1× pen-strep.
2. Staining buffer
Mix 200 μ l of FBS with 9.8 ml PBS, which results in a 2% FBS (v/v) solution in PBS.
3. CD146 staining solution
Mix 10 μ l of Alexa Fluor 647-conjugated anti-CD146 antibody stock solution with 990 μ l of staining buffer, which results 1:100 diluted CD146 antibody solution.
4. Fixative solution

Mix 1 ml of PFA stock solution (16%, v/v) with 3 ml of PBS, which results in a 4% PFA (v/v) solution.

5. Agarose solution

Weight 30 mg of agarose powder and mix it with 1 ml PBS. Place this solution in a oven set at 80°C for at least one hour, in order to melt the agarose. It results in a liquid agarose solution at concentration of 3% (w/v). Prior to cell loading into drops, mix 30 µl of the the 3% (w/v) agarose solution with 70 µl of medium containing 6×10^6 cells. This results in a solution containing cells at a concentration of 6×10^6 cells/ml and agarose at 0.9% (w/v).

6. Permeablization buffer

Mix 500 µl of Triton-X100 with 10 ml PBS, which results in a permeablization buffer containing 0.5% Triton-X100 (v/v).

7. Blocking buffer

Mix 500 µl of FBS with 9.5 ml PBS, which results in a bolocking buffer buffer containing a 5% FBS (v/v) solution.

8. Primary antibodies solution

Mix 10 µl of primary antibody stock solution (anti-COX2, anti-VEGF-A, anti-RUNX-2) with 990 µl of staining buffer, which results 1:100 diluted primary antibody solution.

9. Secondary antibodies solution

Mix 10 µl of Alexa Fluor 594-conjugated secondary antibody stock solution and 20 µl DAPI solution at 14 µM (prepared from 5 mg DAPI resuspended in 10 ml PBS, which stock solution (1.4 mM) is then diluted at 1:100, *i.e.*, 10 µl into 990 µl PBS) with 970 µl of staining buffer, which results in a 1:100 diluted solution of secondary antibodies containging 0.3 µM DAPI.

Acknowledgments

C. Frot is gratefully acknowledged for the help with the microfabrication, and F. Soares da Silva is gratefully acknowledged for the help in flow cytometry. We acknowledge the support of the group of Biomaterials and Microfluidics (BMCF) of the Center for Innovation and Technological Research, as well as the Center for Translational Science (CRT)–Cytometry and Biomarkers Unit of Technology and Service (CB UTechS). The original paper (Sart *et al.*, 2020) has been published in Science Advances (doi: 10.1126/sciadv.aaw7853).

Competing interests

The authors declare that they have no competing interests.

References

1. Amselem, G., Sart, S. and Baroud, C. N. (2018). [Universal anchored-droplet device for cellular](#)

- [bioassays](#). *Methods Cell Biol* 148: 177-199.
2. Caplan, A. I. and Correa, D. (2011). [The MSC: an injury drugstore](#). *Cell Stem Cell* 9(1): 11-15.
 3. Cesarz, Z. and Tamama, K. (2016). [Spheroid Culture of Mesenchymal Stem Cells](#). *Stem Cells Int* 2016: 9176357.
 4. Chang, H., Yang, Q. and Parvin, B. (2007). [Segmentation of heterogeneous blob objects through voting and level set formulation](#). *Pattern Recognit Lett* 28(13): 1781-1787.
 5. Dominici, M., Le Blanc, K., Mueller, I., Slaper-Cortenbach, I., Marini, F., Krause, D., Deans, R., Keating, A., Prockop, D. and Horwitz, E. (2006). [Minimal criteria for defining multipotent mesenchymal stromal cells. The International Society for Cellular Therapy position statement](#). *Cytotherapy* 8(4): 315-317.
 6. Sacchetti, B., Funari, A., Michienzi, S., Di Cesare, S., Piersanti, S., Saggio, I., Tagliafico, E., Ferrari, S., Robey, P. G., Riminucci, M. et al. (2007). [Self-renewing osteoprogenitors in bone marrow sinusoids can organize a hematopoietic microenvironment](#). *Cell* 131(2): 324-336.
 7. Sart, S. and Agathos, S. N. (2018). [Towards Three-Dimensional Dynamic Regulation and In Situ Characterization of Single Stem Cell Phenotype Using Microfluidics](#). *Mol Biotechnol* 60(11): 843-861.
 8. Sart, S., Agathos, S. N., Li, Y. and Ma, T. (2016). [Regulation of mesenchymal stem cell 3D microenvironment: From macro to microfluidic bioreactors](#). *Biotechnol J* 11(1): 43-57.
 9. Sart, S., Tomasi, R. F., Amselem, G. and Baroud, C. N. (2017). [Multiscale cytometry and regulation of 3D cell cultures on a chip](#). *Nat Commun* 8(1): 469.
 10. Sart, S., Tomasi, R. F., Barizien, A., Amselem, G., Cumano, A. and Baroud, C. N. (2020). [Mapping the structure and biological functions within mesenchymal bodies using microfluidics](#). *Sci Adv* 6(10): eaaw7853.
 11. Sart, S., Tsai, A. C., Li, Y. and Ma, T. (2014). [Three-dimensional aggregates of mesenchymal stem cells: cellular mechanisms, biological properties, and applications](#). *Tissue Eng Part B Rev* 20(5): 365-380.